UCRL-PROC-214486

LAWRENCE
LIVERMORE
NATIONAL
LABORATORY

Vlasov Simulations of Trapping and Inhomogeneity in Raman Scattering

D. J. Strozzi (1), M. M. Shoucri (2), A. Bers (1), E. A. Williams (3), A. B. Langdon (3)

(1) Massachusetts Institute of Technology, Cambridge, MA 02139, USA
(2) Institut de Recherche de l'Hydro Québec, Varennes, Qc J3X1S1, Canada
(3) Lawrence Livermore National Laboratory (LLNL), Livermore, CA 94550, USA

15 August 2005

Submitted to *Journal of Plasma Physics* for conference proceedings for 19th International Conference on Numerical Simulation of Plasmas (ICNSP), Nara, Japan, 13 July 2005.

Vlasov Simulations of trapping and inhomogeneity in Raman scattering

D. J. Strozzi[1] * M. M. Shoucri[2] A. Bers[1] E. A. Williams[3]
A. B. Langdon[3]
[1]Massachusetts Institute of Technology, Cambridge, MA 02139, USA
[2]Institut de Recherche de l'Hydro Québec, Varennes, Qc J3X1S1, Canada
[3]Lawrence Livermore National Laboratory (LLNL), Livermore, CA 94550, USA

14 August 2005

Abstract

We study stimulated Raman scattering (SRS) in laser-fusion conditions with the Eulerian Vlasov code ELVIS. Back SRS from homogeneous plasmas occurs in sub-picosecond bursts and far exceeds linear theory. Forward SRS and re-scatter of back SRS are also observed. The plasma wave frequency downshifts from the linear dispersion curve, and the electron distribution shows flattening. This is consistent with trapping and reduces the Landau damping. There is some acoustic ($\omega \propto k$) activity and possibly electron acoustic scatter. Kinetic ions do not affect SRS for early times but suppress it later on. SRS from inhomogeneous plasmas exhibits a kinetic enhancement for long density scale lengths. More scattering results when the pump propagates to higher as opposed to lower density.

1 Introduction and Code Model

Laser-plasma interactions must be controlled for inertial fusion to succeed. This paper examines stimulated Raman scattering (SRS), or the parametric coupling of a pump light wave (the laser, mode 0) to a daughter light wave (mode 1) and an electron plasma wave (EPW, mode 2). Kinetic effects, such as electron trapping, in the daughter EPW are seen to be important in back SRS (BSRS). 1-D kinetic simulations presented here show BSRS much greater than coupled-mode theory for both homogeneous and inhomogeneous plasmas. Strong nonlinearity and non-thermal electron distributions are seen to result.

ELVIS [1] is a 1-D Eulerian Vlasov code that evolves the distribution function f_s ($s =$ species; e for electrons) on a fixed phase-space grid. It uses operator splitting for the time advance [2], [3] and cubic spline interpolation for shifting f_s in position (x) and momentum (p_x). Light waves are linearly polarized in y. The ions can be immobile or kinetic. The governing equations are

$$\left[\partial_t + (p_x/m_s)\partial_x + (Z_s e)\left(E_x + v_{ys}B_z\right)\partial_{p_x}\right] f_s = \nu_{Ks}\left(x\right)\left(n_s \hat{f}_{0s} - f_s\right) \tag{1}$$

$$\partial_x E_x = \frac{e}{\varepsilon_0}\sum_s Z_s n_s \qquad\qquad m_s \partial_t v_{ys} = e Z_s E_y \tag{2}$$

*dstrozzi@mit.edu. Present address: LLNL.

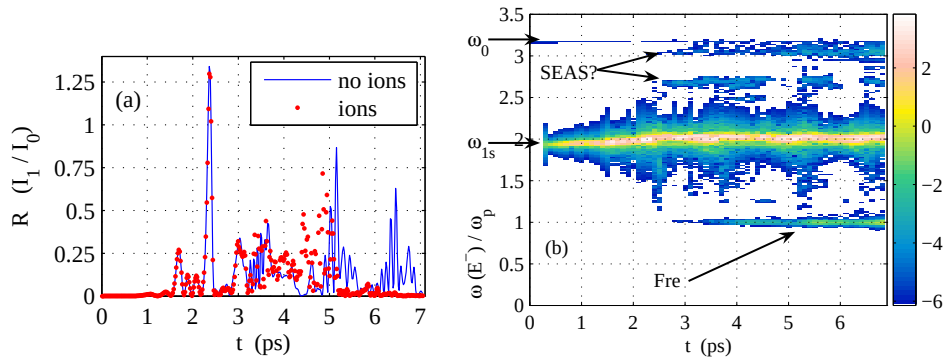

Figure 1: (a) Reflectivity for homogeneous run with immobile (solid curve) and kinetic ions (dotted curve) . (b) Spectrum of reflected light for immobile ions. "Fre" and "SEAS?" label BSRS re-scatter and possible electron acoustic scattering.

$$(\partial_t \pm c\partial_x)\, E^{\pm} = -\frac{e}{\varepsilon_0}\sum_s Z_s n_s v_{ys} \qquad\qquad E^{\pm} \equiv E_y \pm cB_z \tag{3}$$

A number-conserving Krook relaxation operator is included, with relaxation rate $\nu_{Ks}(x)$ and equilibrium Maxwellian $\hat{f}_{0s}$ ($\int dp\ \hat{f}_{0s} = 1$). We use a large $\nu_{Ks} \sim 0.2\omega_p$ ($\omega_p^2 = n_0 e^2/(\epsilon_0 m_e)$) at the edges of the finite density profile to absorb plasma waves generated by SRS and prevent reflection. A nonzero central value of ν_{Ks} can also mimic sideloss from a laser speckle. We advance $E^{\pm}$ without dispersion by shifts of one x gridpoint, which imposes $dx = c\ dt$.

2 Simulations Results

We simulate a pump laser with $\lambda_0 = 351$ nm (vacuum) and intensity $I_0 = 2\times 10^{15}$ W/cm^2 impinging from the left (E^+ contains the pump) on a finite plasma with a flat central region 75.1 μm wide of density $n_0 = 0.1 n_c$ (critical density $n_c = n_0\omega_0^2/\omega_p^2$) and temperature $T_e = 3$ keV. Since Vlasov codes are low-noise there are no numerical fluctuations for SRS to grow from. We therefore inject a counter-propagating seed light wave via E^- with $\lambda_{1s} = 574$ nm and $I_1 = 10^{-5} I_0$. This light has the maximum linear BSRS growth rate and couples to an EPW with $k_2\lambda_D = 0.357$ and a Landau damping rate $\nu_2 = 0.038\omega_p$ ($\lambda_D = v_{Te}/\omega_p$, $v_{Te}^2 = T_e/m_e$). The x grid spacing is $dx = 11.9$ nm, our algorithm requires $dt = dx/c$, and we use a p_x grid spacing $dp = 0.0437 v_{Te} m_e$. SRS is convective for these parameters with a spatial gain rate $\alpha = 0.019\ \mu\text{m}^{-1}$, giving a linear reflectivity $R_{\text{lin}} = 1.72\times 10^{-4}$. The numerical R, shown as the solid curve in Fig. 1(a), is well above this level. R comes in sub-picosecond bursts and has a time average from 1 ps to the run end of $R_{av} = 13.8\%$. $\nu_{Ks} \neq 0$ only at the edges. Repeating the run with a nonzero central ν_{Ks} shows a sharp cutoff of the reflectivity for $\nu_{Ks} \gtrsim 10^{-3}\omega_p$.

The streaked spectrum of reflected light E^- at the left edge is shown in Fig. 1(b). Almost all the energy is contained in BSRS. $\omega_{1s} = 1.93\omega_p$ is the seed light frequency. Initially BSRS occurs at ω_{1s} but upshifts for $t \gtrsim 2$ ps, corresponding to a downshift in ω_2. The weak signal near ω_p labeled "Fre" is the forward Raman re-scatter of upshifted BSRS light. The longitudinal E_x spectrum in Fig. 2(a) reveals the plasma wave at the matching k and ω. Re-scatter is only possible due to the upshift in ω_1, since $\omega_p > \omega_{1s}/2$. The features slightly below ω_0 and slightly above $2.5\omega_p$, labeled "SEAS?", may be related to scattering off the acoustic longitudinal activity discussed below [4]. The transmitted light (E^+) spectrum

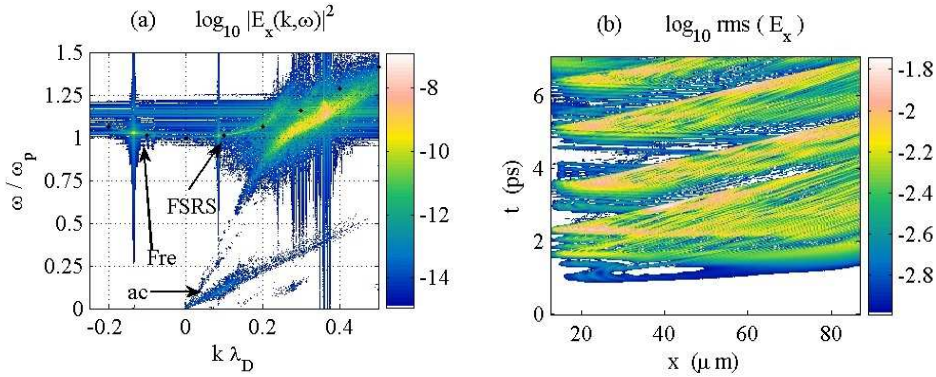

Figure 2: (a) $E_x(k,\omega)$ spectrum for homogeneous, immobile ions run. "Fre", "FSRS", and "ac" label BSRS re-scatter, FSRS, and acoustic activity. The black dots are the linear EPW dispersion curve. (b) rms-averaged $E_x(x,t)$.

(not presented here) shows for $t \gtrsim 3$ ps weak levels of both FSRS and the anti-Stokes line ($\omega = \omega_0 + \omega_p$) of the pump, even though neither of these is externally seeded.

The longitudinal electric field spectrum $E_x(k,\omega)$, depicted in Fig. 2(a), reveals that the BSRS plasma-wave activity is downshifted in frequency from the linear dispersion curve. This is qualitatively consistent with the frequency downshift due to electron trapping [5], and periods of larger downshift correspond to larger EPW amplitude. The downshifted EPW connects with an acoustic-like feature ($\omega \propto k$) that extends to $\omega = 0$. There is another, lower phase velocity acoustic streak, strongest for $\omega \lesssim 0.2\omega_p$. Weak scattering off them may account for the "SEAS?" features in Fig. 1(b). In addition, plasma waves corresponding to FSRS and re-scatter of BSRS occur on the EPW dispersion curve. Fig. 2(b) presents the t and x rms-averaged $E_x(x,t)$, which shows the EPWs occur as a series of wide pulses that move parallel to the laser (that is, to the right). The group velocity matches the slope of the BSRS plasma waves. Near the left edge some pulses propagate opposite the laser.

The electron distribution f_e forms phase-space vortices at the EPW phase velocity $v_{p2} = \omega_2/k_2$ (=0.264c for the linear EPW). The space-averaged $\langle f_e \rangle$, displayed in Fig. 3(a), is flattened due to trapping in this region. Landau damping ($\sim \partial f/\partial v$) is greatly reduced by flattening, which may thereby enhance the reflectivity [6]. When the EPW amplitude is large f_e is quite flat, and only for brief periods ($\lesssim 0.1$ ps) do we see a small bump (region of $\partial\langle f_e\rangle/\partial p_x > 0$) form slightly above v_{p2}.

The run was repeated with kinetic helium ions ($m_i = 4m_p$, $T_i = 750$ eV) and yielded the dotted R in Fig. 1(a). Early in time R is the same for immobile and kinetic ions, while later in time they diverge. For the last 2 ps the reflectivity is very low with kinetic ions. We do not see evidence of Langmuir decay instability (EPW $\rightarrow$ EPW + IAW (ion acoustic wave)) of the EPW or stimulated Brillouin scattering (photon $\rightarrow$ photon + IAW) of the pump. Instead, very high E_x activity develops on the left edge of the box around $t = 5$ ps, involving large ion density fluctuations; BSRS is minimal after this. Most of the spectral power in this activity is concentrated in the FSRS and re-scatter of BSRS features. Further study of the role of ions is underway.

In an inhomogeneous medium, the k matching condition $k_0 = k_1 + k_2$ for a three-wave interaction can only be satisfied at one point. Away from this point the detuning limits the interaction. We performed ELVIS simulations for the same parameters as the homogeneous run with kinetic ions discussed above. However, the central region of the density profile now has a linear gradient extending for 100 μm. We vary the endpoint densities and thereby

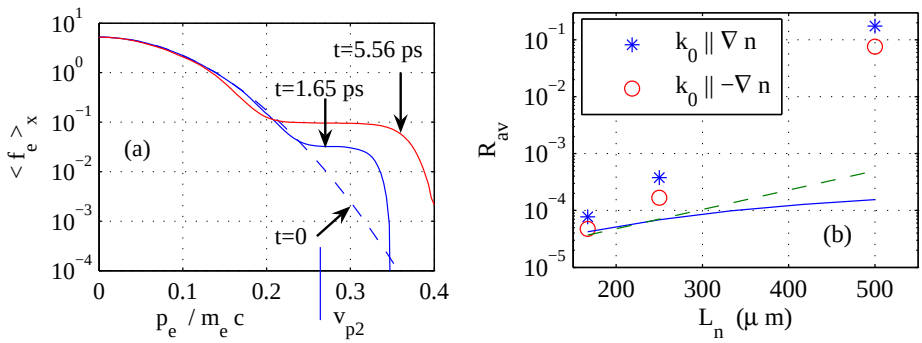

Figure 3: (a) Space-averaged f_e over central 5.62 μm of box for homogeneous, immobile ions run. (b) Average reflectivity for inhomogeneous runs with L_n = (167, 250, 500) μm. (Solid, dashed) curves are the coupled-mode (strong damping limit, Rosenbluth undamped) steady-state R.

change the density scale length $L_n = n/(dn/dx)$. The reflectivities for several L_n are shown in Fig. 3(b), for the pump propagating toward higher and lower densities. Also plotted is the steady-state R predicted from the coupled-mode equations, solved in the limit of strong damping for the EPW (solid curve) as well as the Rosenbluth undamped result (dashed curve). Both coupled-mode calculations give the same R for both directions of pump propagation, yet the simulation consistently shows higher R for $\vec{k}_0 || \nabla n$. We are formulating a theory to explain the high R and the role of pump propagation direction.

3 Conclusions

Vlasov simulations of SRS show strong enhancement of the scattering over coupled-mode predictions for both homogeneous and inhomogeneous plasmas. The resulting plasma waves do not satisfy the linear dispersion relation. The electron distribution shows large trapping and flattening. The role of sideloss and ions need to be further examined, and analytic models that explain these findings need to be developed.

This work was supported by the US Dept. of Energy under grant No. DE-FG02-91ER54109 at MIT and under contract No. W-7405-ENG-48 at LLNL.

References

[1] Strozzi, D., Shoucri, M. and Bers, A. 2004 *Comp. Phys. Comm.* **164**, 156–159.

[2] Cheng, C. Z. and Knorr, G. 1976 *J. Comput. Phys.* **22**, 330–351.

[3] Ghizzo, A., Bertrand, P., et al. 1990 *J. Comput. Phys.* **90**, 431–457.

[4] Montgomery, D. S., Focia, R. J., et al 2001 *Phys. Rev. Lett.* **87**, 155001.

[5] Morales, G. J. and O'Neil, T. M. 1972 *Phys. Rev. Lett.* **28**, 417–420.

[6] Vu, H. X., DuBois, D. F., and Bezzerides, B. 2002 *Phys. Plasmas* **9**, 1745–1763